Study on the quality evaluation metrics for compressed spaceborne hyperspectral data

LI Xiaohui [1], ZHANG Jing [1], LI Chuanrong[1], LIU Yi [2], LI Ziyang [1], ZHU Jiajia [1], ZENG Xiangzhao [1*]

(1. *Key Laboratory of Quantitative Remote Sensing Information Technology*, *Academy of Opto-Electronics*, *Chinese Academy of Sciences*, *Dengzhuang South Road*, *Beijing*, *China*, 100094;
2. *Henan Technical College of Construction*, *Mazhai Economic Development Zone*, *Zhengzhou*, *Henan*, *China*, 450007)

Abstract: Based on the raw data of spaceborne dispersive and interferometry imaging spectrometer, a set of quality evaluation metrics for compressed hyperspectral data is initially established in this paper. These quality evaluation metrics, which consist of four aspects including compression statistical distortion, sensor performance evaluation, data application performance and image quality, are suited to the comprehensive and systematical analysis of the impact of lossy compression in spaceborne hyperspectral remote sensing data quality. Furthermore, the evaluation results would be helpful to the selection and optimization of satellite data compression scheme.

Key words: hyperspectral data; lossy compression; image quality evaluation.

1 Introduction

With the progress in imaging spectrometer, its spatial and spectral resolution increase rapidly, resulting in the boost of image size acquired by the equipment. Limited by the downlink bandwidth, the hyperspectral data acquired by the spaceborne high resolution imaging spectrometer is usually lossily compressed onboard before data transmission. However, when dealing with the lossy data, it is important to define quality metrics or distortion measures, which are able to properly and comprehensively quantify the influence of information loss due to compression on not only the distortion but also on the hyperspectral image quality, the end-user applications, and the on-orbit sensor monitoring. These metrics can be used to ensure that no critical information has been lost during the compression process, and that the scientific value of the original data is preserved [1]. Therefore, to build a thorough quality metric set is also of a growing interest for the current high resolution spaceborne hyperspectral remote sensing (RS) technology.

Originally, the quality evaluation of lossy compressed hyperspectral data takes the advantage of the assessment methods of ordinary still images, such as peak signal noise ratio (PSNR) and mean square error (MSE), which compare the distortion of decompressed image with its original image [1]. By further research, some other methods emerge, such as the method of spectral information divergence (SID)[1], spectral angle (SA) [1], relative spectral quadratic error (RQE)[2] and others. Generally speaking, most of the current quality criteria for the lossy compression of spaceborne hyperspectral data just measure the data change between the original data and the compressed data from the statistical aspect, which cannot thoroughly and systematically reflect the lossy compression's influence to the quality of hyperspectral data.

In this paper, based on the current compression-evaluation methods, the accomplishment of the hyperspectral data application, and the on-orbit data quality monitoring, the quality analysis extent for hyperspectral data compression is extended. Some typical criteria and algorithms are chosen from four aspects including data statistics distortion, sensor performance, data application effect, and image quality. A set of quality evaluation metrics for lossy compressed spaceborne hyperspectral data is built, which is suited to the thorough and systematical analysis of the influence of information loss caused by compression upon the spaceborne hyperspectral data quality and its application results. The metrics are also able to provide support to the option and optimization of the satellite hyperspectral data compression solution.

2 The principle of the metrics

Compared with the traditional single or multiple spectral optical RS image, hyperspectral data is a three dimensional (3-D) image cube composed by intensity images corresponding to each spectrum. On the one hand, the hyperspectral data describes the spatial information of surface feature under each spectrum in different images. On the other hand, the pixel of the same location in these images forms a nearly continuous spectral curve. On the aspect of RS application, the affluent spatial and spectral information contained in hyperspectral data have great potential in accurate feature classification and target recognition. Therefore, as to the analysis and evaluation of the hyperspectral data's compression quality, the analysis of the influence of information loss is necessary to consider the data applications, apart from the traditional comparison methods between original data and decompressed data. Secondly, since the quality and the application effect of the acquired data depend on the status and the performance of RS sensor, on-orbit sensor performance monitoring, which always has been a significant part of the quality analysis & control of the on-orbit satellite RS data, is also an integral aspect in building the quality evaluation metric set for the compressed spaceborne hyperspectral data.

To establish the quality metric set should follow the principle of objectivity, sensitivity and systematism.

Objectivity: introduces data quality related metric criteria which could be calculated and measured quantitatively with mathematic model and algorithms.

Sensitivity: selects the metric criteria which could show sensitive reflection by the impact of the compression algorithm or the change of compressed parameter.

Systematism: from different angle or level, thoroughly and systematically reflects the influence of information loss from data compression upon hyperspectral data and application.

Based on the above principle and according to the hyperspectral satellite data's feature and the application requirements, the criteria option and the construction of the quality evaluation metric set for the compression of spaceborne hyperspectral data will be illustrated in this paper comprehensively considering data statistical distortion, sensor performance, data application effect and image quality.

3 The evaluation of data statistical distortion

In the aspect of data statistical distortion, the current quality evaluation methods could be used to the compressed hyperspectral data. The difference between original data and decompressed data is analyzed from spatial dimension and spectral dimension.

3.1 The distortion of spatial dimension

As to the distortion of spatial dimension, PSNR is the most common criterion. However, PSNR just analyzes the difference between each pixel, therefore, cannot reflect the structural information change among each image. Zhou Wang etc[9]. come up with the metric criterion of structural similarity image measurement (SSIM), which could effectively describe the structural change between two images and maintain the consistency with the visual perception of human observers[10].

3.1.1 Peak signal noise ratio (PSNR)

PSNR takes the advantage of MSE to describe the overall gray scale difference between the original image and the decompressed image. The definition is shown below:

$$PSNR = 10 \times lg \frac{L^2}{MSE} \tag{1}$$

where L indicates the quantity level of one image. The larger the PSNR is, the less the distortion of the decompressed image will be. When one image is losslessly compressed, PSNR is infinite.

3.1.2 Structral similarity image measurement (SSIM)

SSIM includes the brightness, the contrast and the structural information of original image and decompressed image. The definition is shown below:

$$SSIM = \frac{(2\mu_x\mu_y + C_1)(2\sigma_{xy} + C_2)}{(\mu_x{}^2 + \mu_y{}^2 + C_1)(\sigma_x{}^2 + \sigma_y{}^2 + C_2)} \tag{2}$$

where, μ_x and μ_y respectively determine the mean gray scale of the original image and the decompressed image, σ_x, σ_y and σ_{xy} respectively illustrate the standard deviation and the correlation coefficient of the original and the decompressed image's gray level, C_1、C_2 are insignificant positive number to avoid the occurrence of the denominator being zero or too small, resulting in the unstable phenomenon. SSIM ranges from 0 to 1, the larger the value, the more similarity the two images share. If one image is losslessly compressed, SSIM equals 1.

3.2 The distortion of spectral dimension

The common spectral distortion metrics for hyperspectral data include [5] spectral angle, spectral information divergence, spectral similarity and relative spectral quadratic error.

3.2.1 Spectral angle (SA)

SA defines the angle between two spectral vectors, determining the similarity between two spectrums, the formula is shown below:

$$SA_{x,y} = cos^{-1} \frac{\sum_{k=1}^{K} f(x,y,\lambda_k)\tilde{f}(x,y,\lambda_k)]}{\sqrt{\sum_{k=1}^{K} (f(x,y,\lambda_k))^2 \sum_{k=1}^{K} (\tilde{f}(x,y,\lambda_k))^2}} \tag{3}$$

where $f(x,y,\lambda_k)$ and $\tilde{f}(x,y,\lambda_k)$ respectively denote the pixel value of the original hyperspectral data and the decompressed data in the location of (x, y) and under the spectrum λ_k. The smaller the angle, the more similarity the two spectrums share. Some researches [11] use maximum spectral angle (MSA) to represent the spectrum similarity between the hyperspectral data before and after the compression. However, according to the experiment we conduct, the mean spectral angle ($\overline{\mathrm{SA}}$) is more sensitive upon data compression compared with MSA. The formula of $\overline{\mathrm{SA}}$ is defined below:

$$\overline{SA} = \frac{1}{M \times N} \sum_{x=1}^{M} \sum_{y=1}^{N} SA_{(x,y)} \tag{4}$$

where M and N respectively denote the number of rows and the columns of hyperspectral image.

3.2.2 Spectral information divergence (SID)

SID is usually used to assess the similarity among pixel spectrums. For the compressed hyperspectral data, the maximum spectral information divergence (MSID) is frequently used to evaluate the spectral distortion. The definition is described below:

$$MSID = \max_{(x,y)} \{ p_\lambda - \tilde{p}_\lambda \ln(\frac{p_\lambda}{\tilde{p}_\lambda}) \}$$
$$p_\lambda = \frac{f(x,y,\lambda)}{|| f(x,y,\bar{\lambda}) ||_1}, \tilde{p}_\lambda = \frac{\tilde{f}(x,y,\lambda)}{|| \tilde{f}(x,y,\bar{\lambda}) ||_1} \tag{5}$$

where $f(x,y,\bar{\lambda})$ and $\tilde{f}(x,y,\bar{\lambda})$ respectively represent the original data vector and the decompressed data vector.

3.2.3 Spectral similarity (SS)

SS describes the similarity two spectrums share. For the compressed hyperspectral data, MSS (maximum spectral similarity) is frequently used to reflect the spectral distortion. The definition is shown below:

$$MSS = \max_{x,y} \{ \sqrt{MSE_{x,y} + (1 - corr_{x,y}^2)^2} \}$$
$$corr_{x,y} = \frac{\sum_\lambda (f(x,y,\lambda) - \mu) \cdot (\tilde{f}(x,y,\lambda) - \tilde{\mu})}{(n_\lambda - 1)\delta_{f(x,y,g)} \cdot \delta_{\tilde{f}(x,y,g)}} \tag{6}$$

where μ and $\tilde{\mu}$ respectively describe the mean spectrum of the original image and the decompressed image.

3.2.4 Relative spectral quadratic error (RQE)

RQE describes the spectral distortion by calculating the relative deviation of each decompressed spectral image's gray level from the original spectral image's mean gray level. In this paper, RQE's mean pixel is used to represent spectral distortion. The definition is below:

$$RQE_{(x,y)} = \frac{\sqrt{\sum_{\lambda} (f(x,y,\lambda) - \tilde{f}(x,y,\lambda))^2}}{\sum_{\lambda} f(x,y,\lambda)} \tag{7}$$

$$\overline{RQE} = \frac{1}{M \times N} \sum_{x=1}^{M} \sum_{y=1}^{N} RQE_{(x,y)}$$

4 The evaluation of sensor performance

The performance analysis for on-orbit imaging of optical sensor includes radiometric, geometric, spatial and spectral property [12]. Among them, the radiometric property depicts sensor's ability to maintain the relative or absolute energy distribution of the ground scene at the imaging moment. The geometric property reflects sensor's capability to keep the relative or absolute location of the targets in one scene. The spatial property indicates sensor's potentiality to maintain the relative scales and details of the ground targets. The spectral property represents sensor's capacity to restore the spectrum distribution of the targets. Since compression exerts insignificant influence upon the geometric property, the main focus is put upon radiometric, spatial and spectral property when establishing the quality evaluation metrics for the lossy compressed spaceborne hyperspectral data.

4.1 Radiometric property

SNR, the absolute radiometric calibration coefficient and the radiometric resolution are the most typical and common criteria for senor's radiometric property.

4.1.1 SNR

SNR is an important analytical parameter for optical sensor's radiometric resolution and detection sensitivity [13]. During the actual operation, the SNR of the spaceborne push-broom linear array optical sensor is usually calculated by the column difference method through estimating the column noise of the image from uniform scene [14].

4.1.2 The absolute radiometric calibration coefficient

The optical sensor's absolute radiometric calibration coefficient includes gain (G) and bias (B), which represents the numeric relationship between the digital number (DN) of the sensor's output signal and the ground feature's luminance (L) in sensor aperture. It is the premise for the quantitative application of RS information [15]. The on-orbit absolute radiometric calibration coefficient is usually calculated by the reflectance based method [16-18].

4.1.3 Radiometric resolution

The radiometric resolution determines optical sensor's ability to discern the tiniest radiation difference. For the sensors ranging from the visible light and the short-wave infrared, the radiometric resolution is always denoted as the noise equivalent luminance (NEΔL), the definition is described below:

$$NE\Delta L = \frac{L}{SNR} = \frac{(DN\text{-}B)}{G} \cdot \frac{1}{SNR} \tag{8}$$

The above formula indicates that radiometric resolution is calculated by the SNR and the absolute radiometric calibration coefficient. When the variation pattern is consistent with the SNR and the absolute radiometric calibration coefficient, the two factors can replace the radiometric resolution to indicate the variation pattern.

4.2 Spatial property

The metrics for sensor's spatial property contain the spatial resolution and the modulation transfer function (MTF).

4.2.1 Spatial resolution (SR) [19]

SR reflects how well specific features can be resolved by the sensor. However, there is no standard definition for SR. Ground sample distance (GSD), MTF, ground resolvable distance (GRD) and others are used to represent SR. Since GSD is only associated with the sensor's height and CCD detector size, GRD, which describes the recognition for the minimum distance or target size in one image, is usually obtained with the subjective judgment, which cannot meet the objective demands. With further experiments, the MTF value at Nyquist frequency shows regularity under different compression rate, which could indicate the compression impact upon sensor's spatial property.

4.2.2 Modulation Transfer Function (MTF)

MTF defines the variation of the optical sensor's contrast modulation under different spatial frequency. By linking the contrast and the resolution together, it could indicate the contrast modulation loss and the signal spreading of the sensor's imaging of the ground target under each spatial frequency. In order to guarantee the precision of MTF, an optimized knife-edge method in Ref[20]. is recommended in this paper.

4.3 Spectral property

The common parameter to depict the hyperspectral imager's spectral property is the central wavelength and the full width half maximum (FWHM). In the hyperspectral data application, the variation of the central wavelength and the FWHM directly affect the SRF's (spectral response function) retrieval precision, which finally influence the accuracy and the accomplishment of the quantitative application such as classification, identification and others.

To analyze the compression impact upon the sensor's spectral property, the method in Ref. [21] is recommended to calculate the central wavelength's variation ($\triangle\lambda$) and the FWHM's variation ($\triangle$FWHM) of the original hyperspectral data and the decompressed hyperspectral data.

5 The evaluation of data application effect

The effect of data application indicates the application value of RS data, therefore, it is necessary to combine the data compression's quality evaluation and the data's application effect. In the quality evaluation metric set we build for the compressed hyperspectral data, two criteria of spatial interpretability and land surface reflectance are selected for the assessment of data application effect, based on the application feature of the high resolution and high spectral data.

5.1 Spatial interpretability

The evaluation of hyperspectral image's spatial interpretability could refer to the national image interpretability rate standard (NIIRS). By taking the advantage of the general image quality equation (GIQE), the quantitative interpretability can be calculated [22-23].

5.2 Land surface reflectance [24]

The spectral reflectance of land surface is the foundation for the application of the quantified RS information, which is used to describe and unveil the essential of the ground target. The method in Ref[25]. is recommended in this paper to retrieve reflectance in the original and the compressed hyperspectral image.

6 The evaluation of image quality

Image quality determines the effect of image applications and the performance of imaging sensors. By using an array of physical parameter, which could represent the image feature, the evaluation of image quality is realized. The common metric criteria for image quality evaluation include luminance, variance, contrast, spatial frequency, skewness, definition, kurtosis and etc. To guarantee the analysis be objective, systematic and comprehensive, those criteria which show more sensitivity to compression should be selected with high priority when constructing the metrics.

6.1 Luminance, variance, contrast

The mean gray level of all pixels in one image defines the luminance, illustrating the average reflection.

The variance, σ^2 describes the deviation level of each pixel's gray level from the mean gray level, reflecting the affluence of information in one image.

The contrast C depicts the recognition of target in one image, usually defined by the ratio of image variance to luminance.

6.2 Spatial frequency and skewness

Spatial frequency (SF) represents the distribution of gray level in one image under different spatial frequency. Below is the definition:

$$SF(\lambda_k) = \sqrt{(R_f)^2 + (C_f)^2}$$

$$R_f^2 = \frac{1}{M \times N}\sum_{x=0}^{M-1}\sum_{y=1}^{N-1}\left[f(x,y,\lambda_k) - f(x,y-1,\lambda_k)\right]^2 \quad (9)$$

$$C_f^2 = \frac{1}{M \times N}\sum_{y=0}^{N-1}\sum_{x=1}^{M-1}\left[f(x,y,\lambda_k) - f(x-1,y,\lambda_k)\right]^2$$

where M and N respectively indicate the number of columns and rows of one image in spectrum λ_k. Skewness describes the deviation of the histogram of one image from the average symmetric shape, representing the radiometric accuracy of one image. The definition is below:

$$SK = \sum \frac{(i-\mu)^3 \times p_i}{\sigma^3} \quad (10)$$

where i denotes the gray level of an image, p_i represents the probability of pixel whose gray level is i.

6.3 Definition

Definition determines the variance of edge's sharpness in an image, reflecting tiny details the image contains. There is numerous ways to calculate the definition of an image, such as the method of gradient function[26], point sharpness[27], reblur[28], and others. By further analysis, we recommend point sharpness method for its more sensitivity. The expression of point sharpness based definition algorithm is shown below:

$$\mathrm{D} = \frac{\sum_{i=1}^{M\times N}\sum_{a=1}^{8}\left|\frac{df}{dx}\right|}{\mathrm{M} \times N} \quad (11)$$

where M and N respectively indicate the number of columns and rows of one image f, df represents the gray scale difference of a pixel's eight-neighbor in one image, and dx represents the distance increment in each pixel.

7 Evaluation results and analysis

Since most of the current spaceborne hyperspectral imagers are the dispersion and the interference type, two types of hyperspectral data are used with a large number of experiments on the establishment of metric set. One is UAV-HSI data (GSD = 0.7m, 400nm-900nm spectrum range, 128 bands, dispersion type) and the other one is HJ1A-HSI data (GSD = 100m, 400nm-900nm spectrum range, 128 bands, interference type). Some experiment data are shown in illustration 1. For the bulk of the section, we take JPEG2000, one of the most common compression methods for spaceborne optical RS data, as an example to depict the metric set we build.

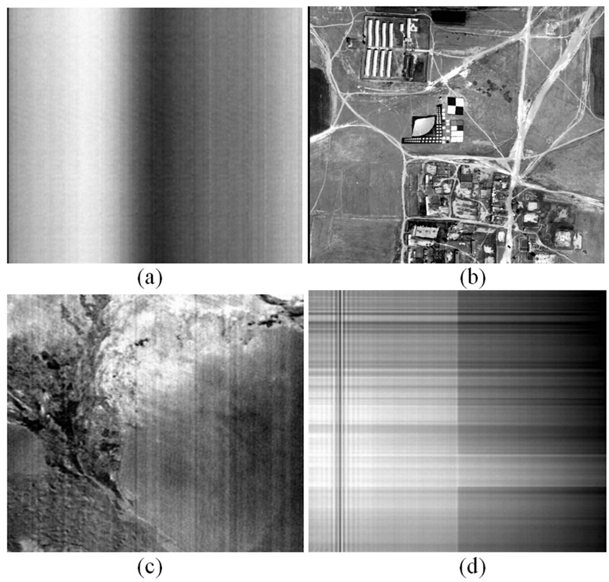

Fig. 1 Experiment data: (a) data 1 the UAV-HSI uniform scene image (b) data 2 the UAV-HSI image (c) data 3 the HJ1A-HSI interferogram (d) data 4 the HJ1A-HSI image from data 3.

Table 1 shows the distortion of the restored image from data 2 and 4 in Fig. 1 compressed by the JPEG2000. It indicates that with the increase of compression rate, PSNR, RQE and MSA rise and SSIM decrease. However, the variance of MSA, MSID and MSS do not show regularity. On the basis of sensitivity principle, PSNR, SSIM, RQE and SA should be included in the metric set to analyze the statistical distortion of the compressed hyperspectral data.

Table 1 The distortion analysis for the compressed data 2 & data 4.

Criteria	*Datasets*	4:1	8:1	10:1	12:1	16:1
PSNR	2	47.7	46.1	45.5	45.0	44.7
	4	47.2	37.9	36.7	36.2	34.8
SSIM	2	0.955	0.941	0.942	0.931	0.926
	4	0.992	0.933	0.909	0.899	0.86
MSA	2	0.06	0.09	0.09	0.09	0.10
	4	1.07	1.05	1.06	1.11	1.20
MSID	2	0.293	0.295	0.294	0.291	0.29
	4	0.01	0.01	0.01	0.01	0.01
MSS	2	78.5	77.7	79.9	77.1	77.6
	4	21.1	50.3	58.4	61.7	72.8
RQE	2	4.21	17.8	19.9	25.86	29.6
	4	12.6	37.38	43.15	45.76	54.19
$\overline{SA}$	2	0.002	0.008	0.019	0.012	0.014
	4	0.011	0.034	0.04	0.042	0.05

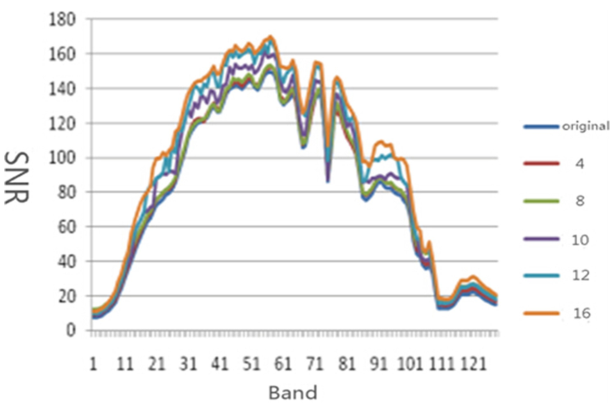

(a)

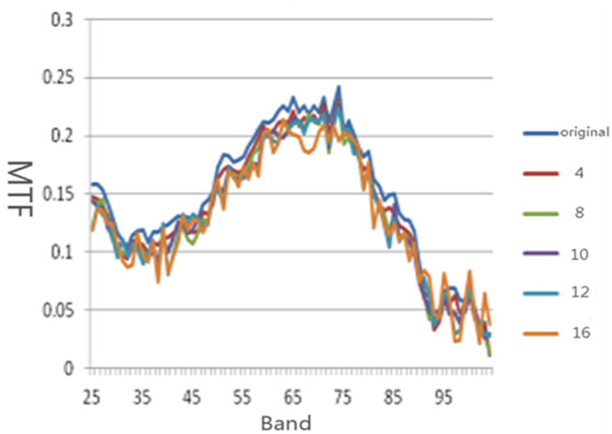

(b)

Fig. 2 The influence of compression upon sensor's radiometric and spatial property by data2: (a) SNR and (b) MTF.

Figure 2 and 3 and Table 2 and 3 demonstrate the influence of JPEG2000 upon the sensor performance and the application effect by using UAV-HSI. Since the previous 24 bands and the last 24 bands of UAV-HSI data are vulnerable to the influence of noise, MTF and NIIRS are of low accuracy and therefore not included in the illustration.

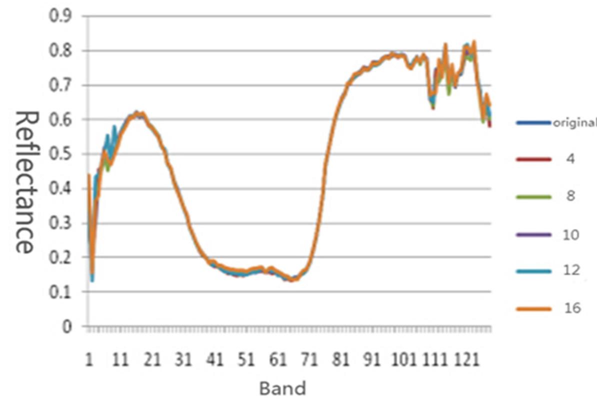

(a)

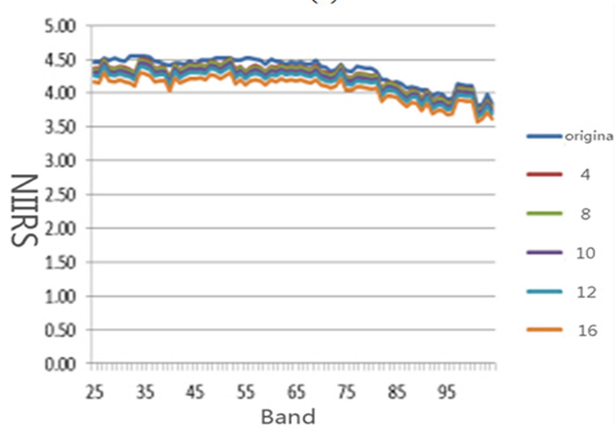

(b)

Fig. 3 The influence of compression upon data's application effect by data2: (a) Surface reflectance and (b) NIIRS.

According to the analysis results, when the compression rate is below 16, JPEG2000 will affect the evaluation of SNR, absolute radiometric calibration coefficient, radiation resolution, MTF and NIIRS and show regular influenced trend as in Fig 2 and 3. Among them, SNR, radiation resolution, MTF and NIIRS are the most influenced metric criteria.

Table 2 The mean percentage of the relative change of sensor performance by data2.

Criteria	4:1	8:1	10:1	12:1	16:1
SNR	5.00	10.11	11.94	17.36	26.83
NEΔL	0.82	5.81	7.31	12.65	18.55
Gain	0.075	0.177	0.221	0.240	0.272
MTF	-7.87	-10.42	-12.25	-13.49	-17.34
NIIRS	-0.05	-0.058	-0.096	-0.141	-0.205
Reflectance	0.005	0.006	0.007	0.007	0.007

Although the analysis results such as table 3, show that JPEG2000 exerts little effect on the sensor's spectral property (central wavelength and FWHM), these two criteria are kept in the metric set considering their intimate relationship with the RS quantitative application and the comprehensiveness of the metrics.

Table 3 The sensor's spectral property by data2.

Criteria	*origin*	4:1	8:1	10:1	12:1	16:1
△λ	0.98	0.96	0.98	0.97	0.92	0.93
△FWHM	-0.01	-0.02	-0.01	-0.02	-0.02	-0.02

Table 4 describes the influence of JPEG2000 upon the image quality by using UAV-HSI and HJ1A-HSI data. As comparison, the influence of the point sharpness based definition algorithm and the reblur definition algorithm are also shown in Table 4.

Table 4 The mean percentage of relative image quality change for data2 & data3.

Criteria	*Datasets*	4:1	8:1	10:1	12:1	16:1
Contrast	UAV-HSI	1.60	1.04	2.10	2.51	4.87
	HJ1A-HSI	0.50	0.08	0.56	0.65	1.21
Spatial frequency (SF)	UAV-HSI	1.80	1.92	2.01	2.12	2.32
	HJ1A-HSI	1.54	2.92	3.42	3.57	4.59
Skewness	UAV-HSI	3.91	4.49	4.91	5.66	6.12
	HJ1A-HSI	2.35	3.37	7.12	9.42	14.7
Definition (Point sharpness)	UAV-HSI	-1.16	-7.35	-11.8	-13.5	-17.6
	HJ1A-HSI	-1.67	-6.44	-10.8	-14.8	-18.3
Definition (Reblur)	UAV-HSI	-0.21	-0.25	-0.78	-0.98	-1.23
	HJ1A-HSI	-1.17	-2.12	-2.80	-1.07	-1.56

According to the analysis, within the 16:1 compression rate, the corresponding relative variance percentages are all less than 5%. Therefore, JPEG2000 exerts tiny influence upon the contrast and the spatial frequency. Upon the image definition, the influence of the point sharpness based definition algorithm is more sensitive than the reblur definition algorithm. For the interference type of hyperspectral data, outside the 12:1 compression rate, JPEG2000 influences much upon skewness. Based on the above analysis, we choose skewness and definition, calculated by the point sharpness based algorithm, to be included in the metric set for the influence of compression upon the image quality.

8 Conclusion

On the basis of deep analysis on the evaluation of the compression of spaceborne hyperspectral data and by following the principle of objectivity, sensitivity and systematism, some proper metric criteria and their corresponding algorithms are chosen. An initial quality evaluation metric set for compressed spaceborne hyperspectral data is built from the aspects of data statistical distortion, the sensor performance, the data application effect and the image quality. Table 5 shows the metric set. The data analysis for JPEG2000 and CCSDS compression schemes indicates that the metric set is suited to the systematical analysis of the influence of compression algorithm upon the quality of the hyperspectral RS satellite data, and is able to provide reference to the option and the optimization of the compression algorithm and compression solution for the hyperspectral data.

Table 5 Quality Evaluation Metric set for the Compressed Spaceborne Hyperspectral Data.

<table>
<tr><td rowspan="7">Quality Evaluation Metric set for the Compressed Hyperspectral Data</td><td rowspan="2">Data Statistical Distortion</td><td>Image Distortion</td><td>Peak Signal Noise Rate(PSNR)
Structure Similarity Image Measurement(SSIM)</td></tr>
<tr><td>Spectral Distortion</td><td>Mean Spectral Angle(SA)
Relative Spectral Quadratic Error(RQE)</td></tr>
<tr><td rowspan="3">Sensor Performance</td><td>Radiation Property</td><td>Signal Noise Rate(SNR)
Absolute Radiometric Calibration Coefficient</td></tr>
<tr><td>Space Property</td><td>MTF</td></tr>
<tr><td>Spectrum Property</td><td>Central Wavelength FWHM</td></tr>
<tr><td>Data Application Effect</td><td colspan="2">NIIRS Surface Reflectance</td></tr>
<tr><td>Image Quality</td><td colspan="2">Skewness Definition</td></tr>
</table>

ACKNOWLEDGMENT

This work was supported by the Chinese 863 Plan Program under Grant 2012AA121504.

References

[1] CHRISTOPHE E, LEGER D, MAILHES C. Quality Criteria Benchmark for Hyperspectral Imagery [J]. Geoscience & Remote Sensing IEEE Transactions on, 2005, 43(9):2103 - 2114.

[2] MAILHES C, VERMANDE P, CASTANIE F. Spectral image compression [J]. Journal of Optics, 1990, 21(3):121-132.

[3] KUMAR S, GHOSH J, CRAWFORD M M. Hierarchical Fusion of Multiple Classifiers for Hyperspectral Data Analysis [J]. Pattern Analysis & Applications, 2002, 5(2):210-220.

[4] ZHOU Y, TIAN Q. Image Quality Evaluation of EO-1 Hyperion Sensor [J]. Geo-Information Science, 2008, 10(5):678-683.

[5] PEARLMAN A J, SEGAL C, LIAO L B, et al. Development and operations of the EO-1 Hyperion Imaging Spectrometer [J]. Earth Observing Systems V, 2000, 4135:43--253.

[6] YARBROUGH S, CAUDILL T R, KOUBA E T, et al. MightySat II.1 hyperspectral imager: summary of on-orbit performance [C]. International Symposium on Optical Science and TechnologyInternational Society for Optics and Photonics, 2002.

[7] ZHONG S. HJ-1A/1B Satellites In-orbit Performance Evaluation [J]. Spacecraft Engineering, 2009.

[8] ZHAO B C, Yang J F, Chang L Y, et al. Optical Design and On-orbit Performance Evaluation of The Imaging Spectrometer for Chang´e-1 Lunar Satellite [J]. Acta Photonica Sinica, 2009, 38(3):479-483.

[9] WANG Z, BOVIK A C, SHEIKH H R, et al. Image quality assessment: from error visibility to structural similarity [J]. IEEE Trans Image Process, 2004, 13 (4):600-612.

[10] WANG Z, SIMONCELLI E P, AND BOVIK A C. Multiscale structural similarity for image quality assessment. Signals [C]. Systems and Computers, 2004. Conference Record of the Thirty-Seventh Asilomar Conference on. IEEE, 2003, 2, 1398-1402.

[11] HYVÄRINEN A, KARHUNEN J, OJA E. Independent component analysis, John Wiley & Sons, New York (2004).

[12] LEACHTENAUER J C, R. DRIGGERS G. Surveillance and reconnaissance imaging systems: modeling and performance prediction, Artech House, Boston (2001).

[13] ZHU B, WANG X, LI Z, et al. A new method based on Spatial Dimension Correlation and Fast Fourier Transform for SNR estimation in remote sensing images [C]. Geoscience and Remote Sensing Symposium (IGARSS), 2013 IEEE InternationalIEEE, 2013:4114-4117.

[14] PASCAL V, CHAFFAUT F X, KUBIK P, et al. A new method for in-flight radiometric noise assessment: application to SPOT5 [C]. Remote SensingInternational Society for Optics and Photonics, 2004:268-279.

[15] LI C R. The Comprehensive Validation System & Technology of Unmanned Aerial Vehicle Remote Sensing, Beijing: Science Press, Beijing (2014).

[16] GUO J N, MIN X J, QIAO-YAN F U, et al. The In-flight Absolute Calibrations for CBERS-02 CCD and SPOT-4 HRVIR1 Sensors at Dunhuang Test Site and the Comparison based on Their Coefficients[J]. Journal of Remote Sensing, 2006, 10(5):624-629.

[17] SLATERP N, BIGGAR S F, HOLM R G., et al. Reflectance- and radiance-based methods for the in-flight absolute calibration of multispectral sensors[J]. Remote Sensing of Environment, 1987, 22:11-37.

[18] DINGUIRARD M, SLATER P N. Calibration of Space-Multispectral Imaging Sensors: A Review [J]. Remote Sensing of Environment, 1999, 68(98):194-205.

[19] PAGNUTTI M, BLONSKI S, CRAMER M, et al. Targets, methods, and sites for assessing the in-flight spatial resolution of electro-optical data products[J]. Canadian Journal of Remote Sensing Journal Canadien De Télédétection, 2010, 36(5):583-601.

[20] LI X, JIANG X, ZHOU C, et al. An analysis of the knife-edge method for on-orbit MTF estimation of optical sensors[J]. International Journal of Remote Sensing, 2010, 31(1718):4995-5010.

[21] WANG T, YAN G, REN H, et al. Improved Methods for Spectral Calibration of On-Orbit Imaging Spectrometers[J]. Geoscience & Remote Sensing IEEE Transactions on, 2010, 48(11):3924-3931.

[22] KIM T, KIM H, KIM H. S. Image-Based Estimation and Validation of NIIRS for High-Resolution Satellite Images [J]. The International Archives of the Photogrammetry, Remote Sensing and Spatial Information Sciences, 2008, 37(B1), 1-4.

[23] LEACHTENAUER J C, MALILA W, IRVINE J, et al. General image-quality equation for infrared imagery[J]. Appl Opt, 2000, 39(26):4826-4828.

[24] DUAN S B, Li X L, Tang B H, et al. Land Surface Reflectance Retrieval from Hyperspectral Data Collected by an Unmanned Aerial Vehicle over the Baotou Test Site [J]. PLOS ONE 8(6): e66972.

[25] LI S S, CHEN L F, TAO J H, et al. Retrieval and Validation of the Surface Reflectance using HJ-1 CCD data[J]. Spectroscopy and Spectral Analysis, 2011, 31(2), 516-520.

[26] ESKICIOGLU A M, FISHER P S. Image quality measures and their performance [J]. IEEE Trans. on Communications, 1995, 43(12), 2959-2965.

[27] WANG H N, ZHONG W, WANG J, et al. Research of Measurement for Digital Image Definition[J]. Journal of Image and Graphics, 2004, 9(7), 828-831.

[28] CRETE F, DOLMIERE T, LADRET P, et al. The Blur Effect: Perception and Estimation with a New No-Reference Perceptual Blur Metric[J]. Human Vision and Electronic Imaging, Proceeding of the SPIE, 2007, 6492, 64920I.1-64920I.11.

Authors' Biographies

LI Xiaohui, born in 1971. She received BSc in 1994 and MSc in 1997, both from University of Sciences and Technology of China. Now she is a professor in Key Laboratory of Quantitative RS Information Technology, Academy of Opto-Electronics, Chinese Academy of Sciences. Her research interests lie in the fields of quality analysis of RS data, RS data processing and RS data compression.

E-mail: xhli@aoe.ac.cn.

ZHANG Jing, born in 1986. She received MSc in 2013 Key Laboratory of Quantitative RS Information Technology, Academy of Opto－Electronics, Chinese Academy of Sciences. Now she is a research assistant in Key Laboratory of Quantitative RS Information Technology, Academy of Opto－Electronics, Chinese Academy of Sciences. Her research interests lie in the fields of quality analysis of RS data.

E−mail: zhangjing@aoe.ac.cn.

LI chuanrong, born in 1956, major in signal and information processing. He is now the director of Key Laboratory of Quantitative RS Information Technology, Academy of Opto－Electronics, Chinese Academy of Sciences. His research interests include ground system of RS satellite, spatial technology in disaster reduction and management, signal and image processing and et al.

E−mail: crli@aoe.ac.cn.

LIU Yi, born in 1987. Now she is a lecturer in Henan Technical College of Construction. Her research interests lie in the fields of image processing.
E-mail: zxwone@qq.com.

LI Ziyang, born in 1977. He is now a deputy director of the Key Laboratory of Quantitative RS Information Technology, Academy of Opto－Electronics, Chinese Academy of Sciences. His research interests include aerospace ground system development and earth observation image processing and information extraction.
E-mail: zyli@aoe.ac.cn

ZHU Jiajia, born in 1982. She received MSc in 2006 from Xi'an Institute of Optics and Precision Mechanics of Chinese Academy of Sciences. Now she is an engineer in Key Laboratory of Quantitative RS Information Technology, Academy of Opto－Electronics, Chinese Academy of Sciences. Her research interests lie in the fields of EO application system and database design.
E-mail: jjzhu@aoe.ac.cn

ZENG Xiangzhao , male, born in 1989. He received MSc in 2014 from Key Laboratory of Quantitative RS Information Technology, Academy of Opto-Electronics, Chinese Academy of Sciences. Now He is a PhD candidate in Key Laboratory of Quantitative RS Information Technology, Academy of Opto-Electronics, Chinese Academy of Sciences. His research interests lie in the fields of LiDAR technology and RS data processing.
E-mail: xiangzhao89@126.com.